Unimorph deformable mirror for space telescopes: design and manufacturing

Peter Rausch,* Sven Verpoort, and Ulrich Wittrock

Photonics Laboratory, Münster University of Applied Sciences, Stegerwaldstraße 39, 48565 Steinfurt, Germany
**rausch@fh-muenster.de*

Abstract: Large space telescopes made of deployable and lightweight structures suffer from aberrations caused by thermal deformations, gravitational release, and alignment errors which occur during the deployment procedure. An active optics system would allow on-site correction of wave-front errors, and ease the requirements on thermal and mechanical stability of the optical train. In the course of a project funded by the European Space Agency we have developed and manufactured a unimorph deformable mirror based on piezoelectric actuation. The mirror is able to work in space environment and is designed to correct for large aberrations of low order with high surface fidelity. This paper discusses design, manufacturing and performance results of the deformable mirror.

OCIS codes: (010.1080) Active or adaptive optics; (350.6090) Space optics; (120.6085) Space instrumentation; (110.6770) Telescopes.

References and links

1. D. Coulter, "Technology development for the Next-Generation Space Telescope: an overview," Proc. SPIE **3356**, 106–113 (1998).
2. S. Verpoort, P. Rausch, and U. Wittrock, "Characterization of a miniaturized unimorph deformable mirror for high power cw-solid state lasers," Proc. SPIE **8253**, 825309 (2012).
3. J. W. Hardy, J. E. Lefebvre, and C. L. Koliopoulos, "Real-time atmospheric compensation," J. Opt. Soc. Am. **67**(3), 360–369 (1977).
4. G. Vdovin and P. M. Sarro, "Flexible mirror micromachined in silicon," Appl. Opt. **34**(16), 2968–2972 (1995).
5. S. Verpoort and U. Wittrock, "Actuator patterns for unimorph and bimorph deformable mirrors," Appl. Opt. **49**(31), 123034 (2010).
6. S. Verpoort, P. Rausch, and U. Wittrock, "Novel unimorph deformable mirror for space applications," in *Proceedings of the 9th International Conference on Space Optics (ICSO),* Ajaccio, Corse (2012).
7. L. D. Landau and E. M. Lifshitz, *Theory of Elasticity* (Pergamon, 1970).
8. D. Damjanovic, "Ferroelectric, dielectric and piezoelectric properties of ferroelectric thin films and ceramics," Rep. Prog. Phys. **61**(9), 1267–1324 (1998).
9. J. Ma, Y. Liu, T. He, B. Li, and J. Chu, "Double drive modes unimorph deformable mirror for low-cost adaptive optics," Appl. Opt. **50**(29), 5647–5654 (2011).
10. R. Bastaits, D. Alaluf, M. Horodinca, I. Romanescu, I. Burda, G. Martic, G. Rodrigues, and A. Preumont, "Segmented bimorph mirrors for adaptive optics: segment design and experiment," Appl. Opt. **53**(29), 6635–6642 (2014).
11. G. Cheriaux, J.-P. Rousseau, F. Burgy, J.-C. Sinquin, J.-M. Lurçon, and C. Guillemard, "Monomorph large aperture adaptive optics for high peak-power femtosecond lasers," Proc. SPIE **6584**, 658405 (2007).
12. H. Cao and A. G. Evans, "Nonlinear deformation of ferroelectric ceramics," J. Am. Ceram. Soc. **76**(4), 890–896 (1993).
13. F. Lowrie, M. Cain, M. Stewart, and M. Gee, "Time dependent behavior of piezo-electric materials," National Physics Laboratory Management Ltd., Teddington, Middlesex, UK, NPL Rep. SMMT (A) **151** (1999).
14. R. Fabbro, P. Peyre, L. Berthe, and X. Scherpereel, "Physics and applications of laser-shock processing," J. Laser Appl. **10**(6), 265–279 (1998).
15. J. C. Wyant and K. Creath, "Basic wavefront aberration theory for optical metrology," in Applied Optics and Optical Engineering, Vol. XI, Chap. 1 (Academic, 1992).

1. Introduction

The design of space telescopes with large primary mirrors calls for structures that are lightweight and provide high surface fidelity at the same time. Mirror mass and size are

#242057 Received 29 May 2015; revised 30 Jun 2015; accepted 30 Jun 2015; published 17 Jul 2015

ultimately limited by the constraints imposed by the launch vehicle. The conventional method to produce optics with high surface fidelity is precluded, since it relies on the use of thick mirror substrates which provide the rigidity needed to maintain the mirror's surface figure. A segmented primary allows larger apertures, but phasing and alignment of the individual segments is challenging and introduces another source of wave-front error.

Active optics is one key element in the implementation of large space optics. Active optics allows for on-site correction of aberrations, and eases the requirements on mechanical stability, thus reducing weight of the supporting structures. The technology development plan for the Next Generation Space Telescope (which has become the James Webb Space Telescope) underlines the importance of active optics in space, denoting cryogenic deformable mirrors and wave-front sensing as two major needs for the optical telescope assembly [1].To successfully operate a deformable mirror in a space telescope, the mirror must be compliant with vacuum, a large temperature range, cosmic irradiation, and vibrations imposed by the launch vehicle. The requirements of the European Space Agency (ESA) demand an operational temperature range from 100 K to 300 K, therefore an athermal design is mandatory. We have designed and manufactured a deformable mirror with a 50 mm aperture that meets these requirements. Section 2 of this paper describes the design considerations, section 3 outlines the manufacturing process, and the last section presents results regarding phase stroke and phase fidelity of the deformable mirror.

2. Design considerations

The mirror concept is based on the unimorph principle. We have developed and refined the design over many years. Initially intended to be used in high power laser applications, heat management was a major consideration during the development of the deformable mirror [2]. The mirror's ability to maintain its shape during a change of ambient temperature renders the design suitable for the demanded operation temperature range from 100 K to 300 K. The shaping of unimorph mirrors is induced by in-plane forces. In contrast to the more common actuation principle using out-of-plane forces (e.g. piezo stacks [3], electrostatic actuation [4] etc.), the unimorph principle has no need for a fixed base plate as support for each actuator. This allows for a lightweight and simple configuration of the mirror, and actuator print-through generated by out-of-plane forces is mitigated. The simple mounting constraints allow customizing the shape of the piezoelectric disc and the design of the electrode pattern without altering the surrounding electrical and mechanical framework.

In the design of deformable mirrors, one has to trade-off surface fidelity and maximum possible stroke. On the one hand, the deforming structure has to be thin to facilitate sufficient stroke with manageable force. On the other hand, thin structures are prone to stress-induced deformation since the bending stiffness of a solid body increases with the third power of its thickness. Figure 1 shows a cross-section of the main mirror structure. It is made of a piezoelectric disc (PIC 151 from PI Ceramic) with a diameter of 84 mm and a thickness of 700 µm, its piezoelectric polarization $\vec{P}_p$ is perpendicular to the mirror surface. The disc is sandwiched between two metallic electrodes, where one electrode serves as a common ground electrode. The electrode on the other side is structured into a 44-electrode keystone pattern with a diameter of 64 mm. The pattern has been optimized numerically to reproduce low order Zernike modes up to the 12th mode with large stroke (e.g. >40 µm in defocus mode, >10 µm in trefoil mode) and diffraction limited surface fidelity at 1 µm wavelength [5]. A prefabricated, super polished and dielectrically coated glass substrate is glued onto the unstructured side of the piezoelectric disc. The use of prefabricated substrates guarantees highly reflective (R > 99.98%) and extremely low scattering optical surfaces, which rival the best available passive optics. The glass substrate is a 550 µm thick disc made of N-BK10 with a diameter of 64 mm.

#242057 Received 29 May 2015; revised 30 Jun 2015; accepted 30 Jun 2015; published 17 Jul 2015

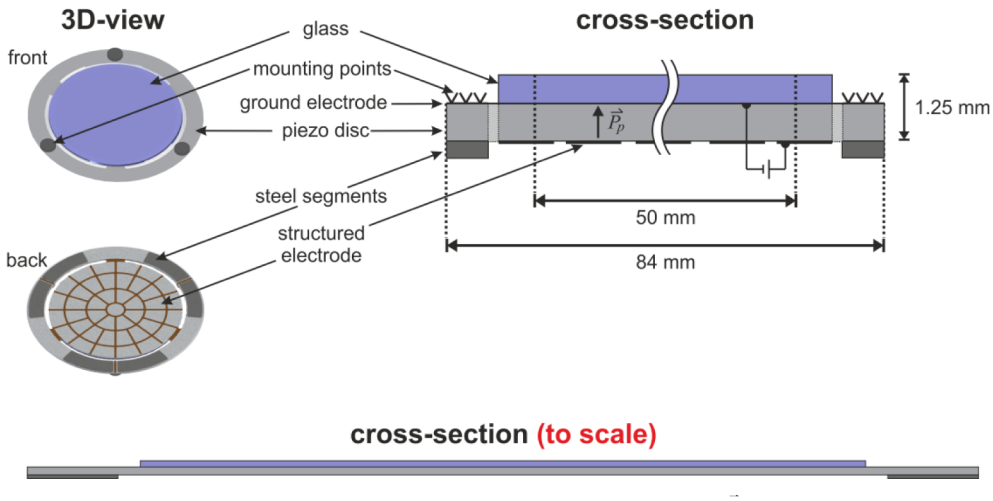

Fig. 1. Top: 3D-view of the main mirror structure along with a cross-sectional view. $\vec{P}_P$: Piezoelectric polarization. Bottom: Cross-sectional view drawn true to scale.

If a voltage is applied to the electrodes, the piezoelectric disc deforms parallel and perpendicular to the piezoelectric polarization (marked by an arrow in Fig. 1)due to the inverse piezoelectric effect. This deformation is proportional to the piezoelectric coefficients d_{33} and d_{31}, respectively. While the deformation parallel to the polarization results in a dimple of only tens of nanometers in height, the deformation perpendicular to the polarization induces stress between the active piezoelectric disc and the passive glass substrate. This stress causes the laminate to deform locally with an amplitude of several micrometers.

Our mirror has an aspect ratio (diameter-to-thickness) of approximately51. Mounting a mirror with such large aspect ratio requires special considerations. The rigidity of the connecting joints has to be chosen carefully. High rigidity is beneficial in terms of dynamic behavior, but might impede the deforming capability of the mirror. In contrast, a soft joint (e.g. a rubber surrounding) allows the mirror to deform almost freely, but would require additional damping stages or a clamping mechanism during launch. Even more important, a soft joint might slowly deform upon changes of ambient temperature or gravitational release. This would lead to an undefined, creep-like behavior of the mirror. Furthermore, the dynamic bandwidth would be reduced significantly due to the low mechanical Q-factor of soft materials. Our design solves the mentioned issues as follows: Three arms have been cut into the piezoelectric disc, as shown on the left side of Fig. 1. The ends of the arms are firmly fixed to three support points, providing high rigidity while allowing the central disc to deform almost freely. Steel segments are glued to the arms as a passive layer. In that way, the arms not only serve as mounting but enable an integrated, monolithic tip/tilt functionality without the need for additional equipment. We use the Fe-/Ni alloy Kovar (material number 1.3917) for the steel segments. Extensive measurements have revealed that the coefficient of thermal expansion (CTE) of Kovar is nearly matched with the CTE of the piezoelectric material PIC 151 [6].Thermal stress as a result of CTE mismatching, which is a constant issue of bimorph and unimorph structures, is mitigated.

3. Manufacturing

3.1 Surface fidelity

The thin, reflectively coated glass substrates initially exhibited a strong spherical deformation. This was caused by coating-induced stress. To compensate for this deformation, a dielectric stress-compensation layer was applied to the opposite side of the glass substrate by the

#242057 Received 29 May 2015; revised 30 Jun 2015; accepted 30 Jun 2015; published 17 Jul 2015

coating vendor on all future glass substrates. The resulting spherical deformation had a peak-to-valley amplitude of 3 µm over the 50 mm aperture. The residual low-order deformation is of mainly astigmatic shape and has a peak-to-valley deviation from best sphere of approximately 0.5 µm, which is very good considering the extreme aspect ratio of the glass disc of over 100.

The unpowered deformation of an assembled mirror can be separated into two parts, the first part containing deformations of low Zernike order, the second part containing deformations with high spatial frequency. Figure 2 depicts the two different deformation domains at the example of a previously manufactured version of our deformable mirror. The total peak-to-valley deviation from the best-fitting sphere in the unpowered state(Fig. 2(a)) is 4.76 µm. In the actively controlled state, the residual peak-to-valley deviation from best sphere is 0.29 µm, and the RMS deviation averaged over the whole surface is 0.04 µm. The largest contribution to the total unpowered deformation of the assembled mirror occurs during the manufacturing process, and is caused by curing-induced stress of the adhesive. This low order deformation of typically astigmatic shape is similar to the first deformation eigenmodes of the deformable mirror. When mechanically stressed, the thin mirror laminate will adapt a shape which represents the equilibrium between external stress and internal energy of deformation [7]. In such thin laminates, even very low stress results in a fairly large deformation. To maintain a good surface fidelity it is crucially important to keep the stress level as low as possible. This also means that non-180° domain wall processes which alter the strain of the piezoelectric material [8] must be kept minimal after curing of the adhesive.

The deformations with high spatial frequency resemble the backside electrode pattern, and are similar in appearance to mechanical actuator print-through. However, in the unimorph actuation principle the actuators induce only negligible stress normal to the mirror; hence print-through cannot arise in that way. Print-through similar to ours is frequently observed in deformable mirrors using the bimorph and unimorph actuation principle with piezoelectric PZT ceramics [9–11], but no thorough explanations are provided. In [10], parametric studies were conducted on the formation of the print-through; the authors conclude that their analysis indicates print-through as inherent to the bimorph actuation principle.

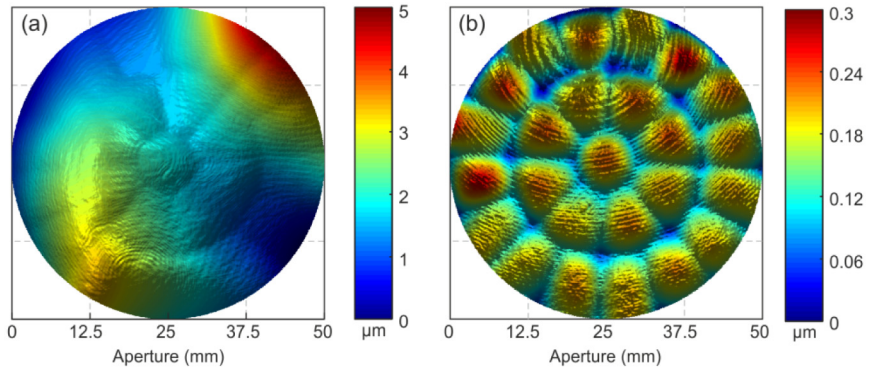

Fig. 2. (a) Initial surface deformation of an early version of our deformable mirror, comprised of high- and low-order deformations. The peak-to-valley deviation from best sphere is 4.76 µm, the RMS surface deviation is 0.81 µm. (b) Surface of the same mirror in actively controlled state with a surface deviation of 0.04 µm RMS. The high-order deformation is clearly seen.

In the following, we offer an explanation of the observed print-through which might help in reducing it. Unlike the mirror concept presented in [10], the print-through in our concept cannot arise from discontinuities of the mechanical geometry, since we use a plain PZT disc, not individual PZT patches. We rather suggest that the root cause is the electromechanical behavior of the used piezoelectric material.

#242057 Received 29 May 2015; revised 30 Jun 2015; accepted 30 Jun 2015; published 17 Jul 2015

Firstly, the piezoelectric disc has to have a non-zero net polarization to facilitate actuation, which is achieved by poling. Ideally, the piezoelectric polarization of the material would be homogeneously oriented. However, this is only possible in single crystals, where a mono domain state can be achieved [8]. In polycrystalline PZT ceramics, each grain is split into domains with different polarization. When poled, the polarization directions of these domains are only oriented within a cone [8], where the axis of the cone resembles the poling direction of the piezoelectric disc. The opening angle of the cone is determined by the crystallographic properties of the used PZT ceramic, typically several degrees.

Even in the poled state, the interplay between internal stresses and internal electric fields results in domains which are not oriented within the poling direction. Additionally, a given state of piezoelectric polarization is not entirely stable. Domains which are oriented unfavorably are readily reoriented by small external influences, while other domains require strong fields to reorient, leading to the well-known hysteretic behavior of such ceramics [12].It is likely that the net polarization of poled piezoelectric discs decreases during the manufacturing process of the deformable mirror. Especially manufacturing steps which involve elevated temperatures, electric fields, and mechanical stress may induce depolarization [13]. If the depolarization involves non-180° domain reorientations, the sample will deform.

After the adhesive, which bonds piezoelectric disc and glass substrate together, is cured, any deformation of the piezoelectric disc will cause the mirror laminate to deform. If the assembled mirror is actuated, the applied electric field will cause deformation due to the inverse piezoelectric effect, but also domain reorientation of the piezoelectric material in the area of the mirror's electrodes. If the newly oriented domains result from non-180° domain wall processes, this reorientation leads to additional deformation. It is important to consider that at least a part of this additional deformation is irreversible and will not entirely vanish in the unpowered state, since it does not originate from piezoelectric actuation but from domain reorientation. The domains in the area of the gap between two electrodes will not reorient during actuation, hence the deformation of the piezoelectric disc within the gaps will differ from the deformation in the area of an electrode. A deformation with opposite sign is observed if the piezoelectric disc is subjected to an electric field in the poling direction before curing the adhesive ("pre-poling"), with the field strength being higher than the field strength used to actuate the mirror.

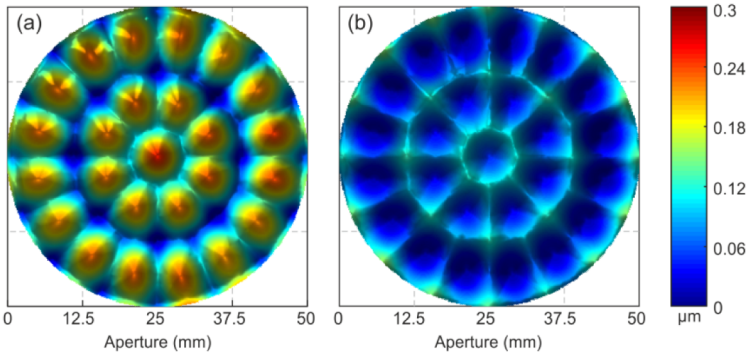

Fig. 3. Numerically calculated surface deviation from flat simulating different strains due to domain reorientation.(a) Positive strain in the area of the mirror electrodes. (b) Negative strain in the area of the mirror electrodes.

We have conducted Finite-Element Method calculations on the electromechanical behavior of our mirror, simulating the local domain reorientation. Figure 3 depicts the residual surface deviation from flat. Deformations of low order have been filtered out to show the influence of local domain reorientation more clearly. Two cases were simulated: reorientation

#242057 Received 29 May 2015; revised 30 Jun 2015; accepted 30 Jun 2015; published 17 Jul 2015

of domains due to actuation, which result in increased net polarization and positive strain in the area of the mirror electrodes (Fig. 3(a)). And, in the second case, loss of net polarization due to strong pre-poling, leading to the inverse behavior (Fig. 3(b)). In both cases, the resulting deformation clearly resembles the back-side electrode pattern, but the signs of the deformation are opposite.

Our numerical results thus indicate that the sign of the print-through can be steered in both directions. Hence, it should be possible to achieve a balance between the two. If the right measure is found, the unimorph deformable mirror can be manufactured without print-through. Figure 4 depicts the residual deviation from best sphere of three different mirror generations which we have manufactured, in chronological order. We were able to reduce the observed print-through with every generation, both in magnitude and in its resemblance to the electrode pattern. The initial deviation from best sphere of approximately 292 nm (40 nm RMS) in the first mirror generation was inverted and reduced to 187 nm (17 nm RMS) in the second generation and 178 nm (19 nm RMS) in the current generation. The last two generations both yield Strehl ratios greater 0.98, whereas the distinctiveness of the print-through is significantly reduced in the latter. As Fig. 4(c) shows, the deformation of this mirror is random and no resemblance to the electrode pattern can be observed. Print-through is thus not inherent to bimorph or unimorph actuation, as also indicated in [11].

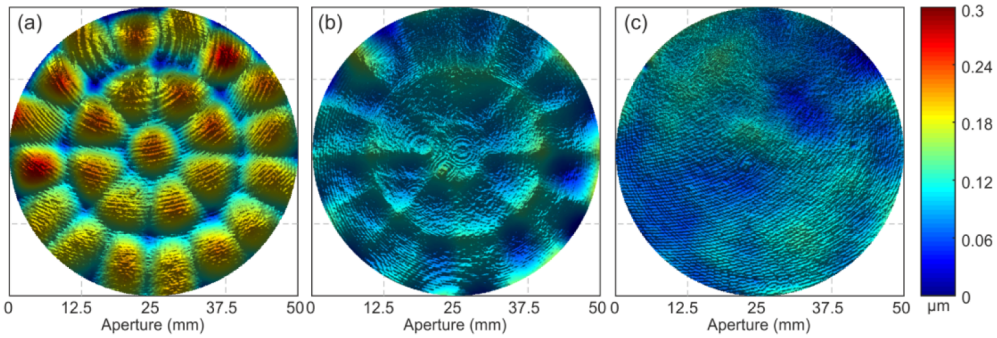

Fig. 4. From left to right: residual surface deviation from best sphere of three successively manufactured deformable mirrors. (a) First mirror generation, manufactured in 01/2013 exhibiting a residual deviation from best sphere of 40 nm RMS. (b) second mirror generation, manufactured in 12/2013. The improved handling of the piezoelectric disc allowed for a residual deviation of 17 nm RMS. (c) Current mirror generation as of 09/2014. The residual deviation from best sphere is 19 nm RMS. The distinct electrode print-through is no longer visible.

3.2 Manufacturing workflow

The piezoelectric disc shave an initial thickness of approximately 1 mm and are furnished with screen-printed silver electrodes at the front side and the back side by the vendor. First, the initial deformation of the discs was measured via white light interferometry. We have measured the surface of 11 such piezoelectric discs. The residual peak-to-valley deviation from best sphere was between 20 µm and 50 µm within the central 50 mm aperture of the disc and consisted mainly of astigmatism.

The electrode on the front side of the piezoelectric disc was abrased and the disc was tempered for 96 hours at 125°C to relieve mechanical stress inside the disc. The disc was then lapped to its final thickness of 700 µm. During the lapping process, emphasis was put on reducing the non-spherical deformation of the piezoelectric disc. However, due to remaining stresses inside the disc, reduction was only possible down to approximately 10 µm to 20 µm peak-to-valley within the 50 mm aperture.

After lapping, a new ground electrode was applied onto the lapped front side by thermal evaporation (PVD – physical vapor deposition). We chose Aluminium as electrode material

#242057 Received 29 May 2015; revised 30 Jun 2015; accepted 30 Jun 2015; published 17 Jul 2015

because it adheres well to the piezoelectric material, and is compatible with the adhesive used to glue the coated glass substrate onto the piezoelectric disc.

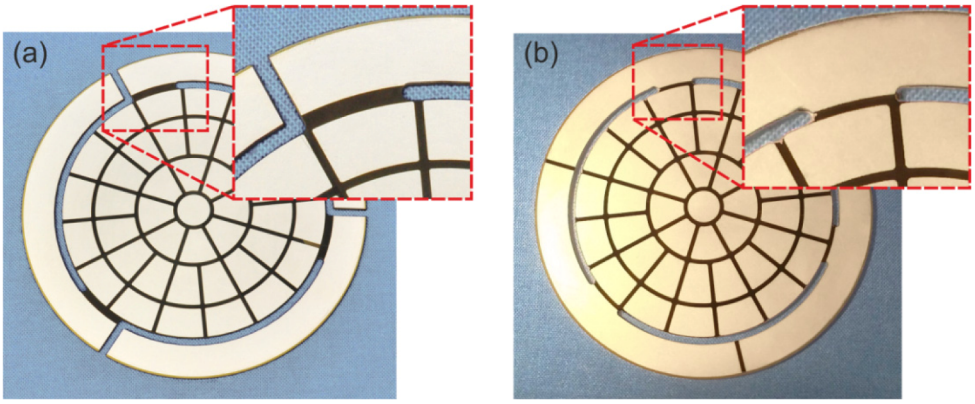

Fig. 5. Detailed view of the two versions of the three-arm piezo structure with the back side electrode pattern.(a) Spiral arm design (b) Bridge design. The insets show the junctions between the central disc and one of the arms in detail.

The electrode on the back side of the disc was structured with a picosecond-laser system (TruMicro 5050, TRUMPF GmbH) into a 44-electrode keystone pattern. Three arms were cut into the disc with the same laser system. We used the picosecond-laser system to avoid any heat affected zone, which could cause localized, heat-induced depolarization of the piezo material. While picosecond laser materials processing creates almost no heat affected zone, the ablation process does create compressive stress. This is used for hardening materials, the technique is known as laser shock peening. The magnitude of the compressive stress created by unconfined laser shock peening is in the order of several 100 MPa [14]. The used PZT ceramic PIC151 exhibits depolarization already at compressive stresses of 100 MPa [12].Depolarized areas within the gaps between the electrodes may contribute to the observed electrode print-through. The edges of the electrode pattern were rounded to avoid high-voltage arcing. In a similar fashion, the edges of the structure were rounded with fillets to reduce mechanical stress concentrations. Two designs of the three arm structure were manufactured; the geometries are depicted in Fig. 5. The spiral arm design (Fig. 5(a)) allows for very large tip/tilt amplitudes of the central disc, but exhibits a low mechanical resonance frequency of 82 Hz in the direction normal to the disc surface. In the bridge design (Fig. 5(b)), the three arm structure is stiffer at the expense of tip/tilt amplitude, thus allowing for higher correction bandwidths (first eigen frequency at approximately 230 Hz) and improved resilience towards vibration loads.

The Kovar steel segments used for tip/tilt actuation were bonded to the arms of the piezoelectric disc using Epo-Tek 353ND.The reflective glass substrate was bonded onto the unstructured front side of the piezoelectric disc with the low-outgassing, space qualified two-component epoxy Epo-Tek 301-2. The epoxy was cured at room temperature for 96 hours to provide stress-free hardening. To mount the main mirror structure into the housing, the arms of the three-arm structure were glued onto a three-point mount. We used an electrically conductive two-component epoxy (Epo-Tek 4110-LV) to ensure electrical connection between the ground electrode and the mounting structure.

#242057 Received 29 May 2015; revised 30 Jun 2015; accepted 30 Jun 2015; published 17 Jul 2015

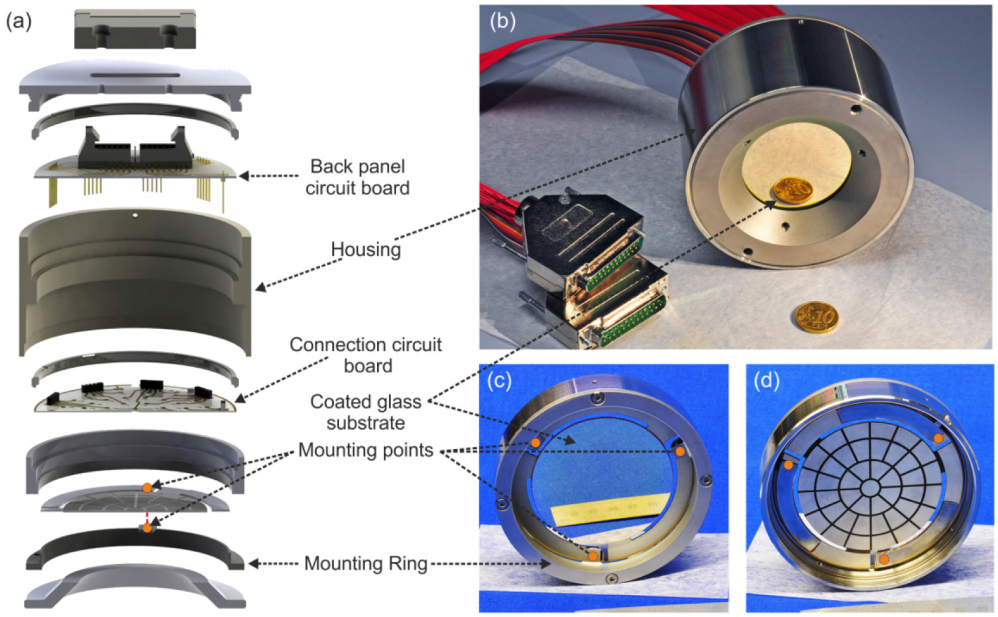

Fig. 6. Deformable mirror assembly.(a) Exploded view. (b) Fully assembled mirror. (c) Front side and (d) back side of the mounted three arm structure.

An image of the assembled deformable mirror along with an exploded view is shown in Fig. 6. All housing parts were made from Kovar to allow for large temperature variations without temperature-induced deformations. The circuit boards facilitating the electric connection were made from Al_2O_3 ceramics with screen-printed circuits. The back side electrodes on the piezo disc were connected to the "connection circuit board" via gold wires with a thickness of 25 µm. The connection circuit board is connected to the back panel circuit board via plugs.

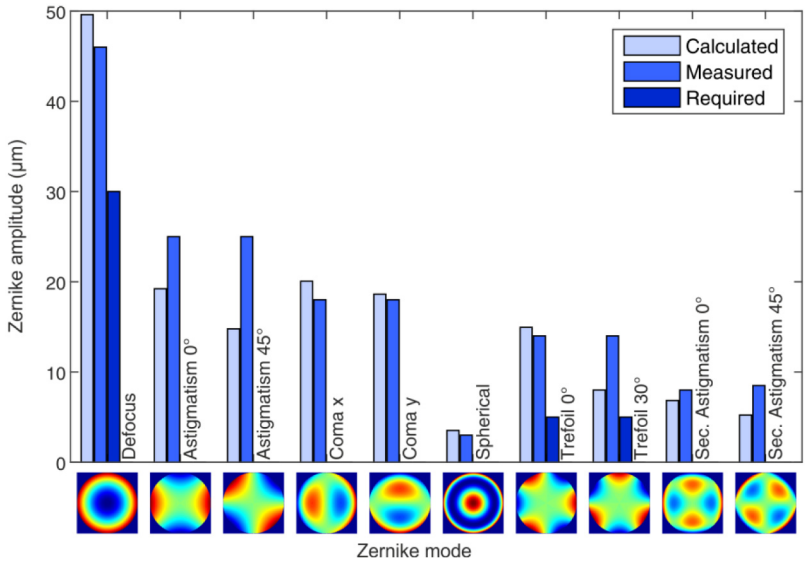

Fig. 7. Comparison of numerically calculated and measured Zernike amplitudes. Each measured amplitude is either voltage or Maréchal limited

#242057 Received 29 May 2015; revised 30 Jun 2015; accepted 30 Jun 2015; published 17 Jul 2015

4. Performance results

To characterize the mirrors, we conducted high resolution interferometric measurements. The Zernike modes Z_1 to Z_{12}were applied to the deformable mirrors in closed-loop operation to determine the maximum amplitudes and the respective surface fidelities. Throughout this paper we use the Zernike notation of Wyant and Creath [15].The loop operation started at amplitudes of 0.5 µm for every Zernike mode. The amplitude was raised in steps of 0.5 µm until one of the following criteria arose: The residual RMS deviation from the target surface exceeded λ/14 (λ = 1064 nm, Maréchal-criterion), or the required voltage exceeded the maximum allowed voltage of +/–400 V. The comparison of numerically calculated and measured maximum Zernike amplitudes is shown in Fig. 7. The measured amplitudes correspond well to the numerically calculated Zernike amplitudes. The strokes exceed ESA's requirements. In defocus mode (Z_3), a stroke of 45 µm was achieved (30 µm required), the trefoil modes ($Z_{9,10}$) were reproduced with a stroke of 15 µm (5 µm required).

5. Summary

In the course of an ESA GSTP-activity we have developed a unimorph deformable mirror with very large stroke and high surface fidelity. The performance of the mirror regarding stroke and surface fidelity exceed ESA's requirements. We were able to reduce the frequently observed residual surface deformation (print-through) observed in this kind of mirror to 17 nm RMS, yielding a Strehl ratio of 0.99. By design, the mirror is suitable to be used in space environment, operating in vacuum and at cryogenic temperatures. We have conducted performance tests in vacuum at cryogenic temperatures, as well as environmental tests. Results from these tests will be reported in a subsequent paper.

Acknowledgments

The authors gratefully acknowledge support for the work presented by the European Space Agency under contract number 4000104030/10/NL/EM.

#242057 Received 29 May 2015; revised 30 Jun 2015; accepted 30 Jun 2015; published 17 Jul 2015